

Research Article

Custom-Built Earth-Based Hypergravity Platform to Study Gravity and Light Tropisms on Soil-Grown Seedlings

Matthew Joseph Dionela, Miguel Alaan, Jaun Raquel Lato, Jacob Reyes, Jasper Matthew Tan, Ronnie Concepcion II* and R-Jay Relano

Department of Manufacturing Engineering and Management, De La Salle University, Manila, Philippines

* Corresponding author. E-mail: ronnie.concepcion@dlsu.edu.ph DOI: 10.14416/j.asep.2025.05.003

Received: 13 January 2025; Revised: 16 February 2025; Accepted: 3 March 2025; Published online: 13 May 2025

© 2025 King Mongkut's University of Technology North Bangkok. All Rights Reserved.

Abstract

Earth-based facilities to generate altered gravity provide valuable tools to study crop resilience and adaptation to non-terrestrial gravity, offering a cost-effective alternative to space-based studies. While centrifuges and clinostats simulate hypergravity and microgravity, respectively, their limited scale often restricts research to small, isolated systems, such as cell cultures or petri-dish seedlings, which lack complex interactions such as those in soil-grown plants. Addressing these limitations, this study aimed to develop a 1-axis hypergravity platform with adjustable chambers designed for soil-grown *Zea mays* seedlings, incorporating controllable gravity, lighting, and irrigation with real-time monitoring through ThingSpeak platform. This platform allowed investigation on how hypergravity (5 g) and photosynthetic photon flux density (6.80–12.95 $\mu\text{mol}/\text{m}^2/\text{s}$) impact maize growth and morphological traits, including main root length (MRL), seminal root count (SRC), dominant seminal root length (DSRL), shoot length (SL), and leaf count (LC). Results showed that 5 g conditions with higher light levels (12.95 $\mu\text{mol}/\text{m}^2/\text{s}$) enhanced root elongation and stable leaf counts, while seedlings in 1 g preferred moderate light (6.80–8.16 $\mu\text{mol}/\text{m}^2/\text{s}$) to avoid growth limitations. Additionally, hypergravity strongly influenced root and shoot growth, promoting root elongation essential for plant stability or anchorage and nutrient uptake. These findings highlight the importance of adjusting gravity and light exposure to optimize growth, providing a basis for future strategies in controlled agricultural systems for terrestrial and extraterrestrial applications.

Keywords: Altered gravity, Controlled environment agriculture, Digital agriculture, Plant adaptation, Space agriculture

1 Introduction

Two of the most vital environmental factors that affect the growth and shape of plants are gravity and light as they influence key physiological processes. Gravitropism is the directional response of plant growth to the gravitational stimulus, as it generally ensures the shoots grow upward and roots downward, optimizing its structural stability and resource acquisition. The central mechanism in gravitropism is auxin redistribution, promoting differential growth and organ curvature as it accumulates asymmetrically [1]. The LAZY1 gene family regulates shoot gravitropism and branch angles, emphasizing the genomic basis of this response [2]. Furthermore,

intracellular trafficking of PIN-FORMED 2 (PIN2) plays a vital role in the transport of auxin during gravitropic responses, where the proper growth direction is affected by the precise localization of PIN2 [3].

On the other hand, phototropism is the directional growth of plants guided by the direction of the light stimulus and is a crucial adaptive process that optimizes the plant's photosynthesis in shoot organs. Blue light photoreceptors, such as phot1 and phot2, initiate signaling to redistribute auxin and determine directional growth responses [4]. The non-phototropic hypocotyl 3 (NPH3) protein is another essential to this coordinating response through linking PIN2-mediated auxin transport and phototropin signaling in roots [5].

Recent studies highlighted that phototropism is critical in both shoots and roots, as it allows the plant to adapt to varying growth and light conditions [6]. These research findings advance bio-inspired technologies and the utilization of artificial light-harvesting systems to optimize light-use efficiency in agricultural applications [7]. Moreover, recent advancements in the study of plant gravitropism and phototropism highlighted the importance of using simulated altered gravity conditions and lights to further explore their impacts on plant growth.

Simulating gravity conditions including partial gravity and hypergravity on Earth is vital for the research advancement not just for space biology but also for agriculture, plant biology, and other branches of research. Microgravity (in the range of $\times 10^{-6} g$) and partial gravity (less than $1 g$ but greater than $0 g$) have been extensively studied for different applications [8]–[10], however, understanding hypergravity is equally essential, as it reveals how plants respond to mechanical forces greater than on Earth, which is vital for preparation for terrestrial applications and space missions [11]. As regards plant growth, hypergravity has been shown to affect key physiological processes such as auxin transport, lignin deposition, and root elongation, which are critical in plant stability and adaptability [12], [13]. These research findings are relevant for space travel where plants must adapt to gravitational pull variation during launch, travel, and extra-terrestrial environments [14].

Altered gravity in space poses substantial challenges relative to plants, such as disrupting fundamental processes such as the interaction of phototropism and gravitropism, which are critical in plant orientation and growth [14]. Hypergravity affects the cellular responses and metabolic pathways, which may enhance or impair plant growth depending on the duration of exposure and intensity of the altered gravitation force [8]. Moreover, considering other research fields, altered gravity environments can affect the stability of other biological products, such as pharmaceuticals like vaccines, potentially reducing their efficacy during space travel or in extraterrestrial colonies [9]. Thus, simulating altered gravity on Earth can provide valuable insights into how biological products and plants might behave in actual extraterrestrial environments, helping researchers and scientists to design more resilient biological and agricultural products for space exploration [12].

Hypergravity is commonly simulated using a centrifuge device, which generates an increase in gravitational pull greater than $1 g$ or Earth's normal

gravity. This device is rapidly rotating objects, creating centrifugal force and acceleration that mimics hypergravity. Centrifuges are commonly utilized in biological, physical, and engineering research to study the impact of altered gravity on living organisms and materials [15], [16]. Another simulation approach involves the combination of centrifuge and clinostats, allowing to mimic the variable gravitational conditions, which expose the system to alternating hyper-microgravity conditions, which are experienced during parabolic flights [17]. These devices enable the researchers to apply external force on biological systems, causing them to adapt to mechanical stress and potentially providing insights into how different organisms may react in extreme terrestrial conditions [18]. However, research and experiments involving hypergravity simulations are often employed in small-scale systems, for instance, the Multi-Sample Incubation Centrifuge (MuSIC) is utilized in small samples such as cell cultures, small plants, or aquatic vertebrates placed in petri dishes, Eppendorf tubes, and multiple well plates [19]. On the other hand, there is already a Large Diameter Centrifuge at the European Space Agency (ESA) center which allows hypergravity research on large samples or plants up to $20 g$ [20]. This represents a significant gap in current research, where the natural soil interactions are absent, thus the effects of hypergravity on soil-grown seedlings remain mostly unexplored. Soil-grown plants exhibit different nutrient intake, root behavior, and overall growth patterns compared to plants grown in artificial ground environments, making it more crucial to study them under altered gravity conditions to obtain more substantial insights into their development. Hypergravity experiments on soil-grown seedlings are important for space and extraterrestrial environments despite the absence of gravity in space because they serve as a model for understanding how plants respond to altered gravitational forces. From the perspective of biology, this can be used for preconditioning for intended space growth, enhanced plant cell wall rigidity and structural integrity before transferring to the actual grow medium in space, and to induce stress resistance and metabolic adaptations even hormone regulation for intensive production. Moreover, during the launch phase of a space shuttle or rocket carrying seeds for potential space agriculture applications, the seeds experience transient hypergravity conditions. Understanding how seeds and seedlings respond to hypergravity can provide insights into their viability and growth potential in space environments. Space

agencies, such as ESA and the National Aeronautics and Space Administration (NASA), employed varying centrifuge or rotating platform designs, making it complicated to compare across the field of astrobotany and space life sciences. ESA's hypergravity simulation platforms have challenges in terms of the centrifuge design standardization depending on the applications that will be experimented and NASA's hypergravity platforms cannot support long-duration experiments.

While centrifuges and clinostats can simulate hypergravity and microgravity, these simulations are often applied to small, isolated systems, which may not replicate the complex interactions found in larger, integrated environments. This restricts insights into how plants or other organisms might fully respond in hypergravity conditions. Moreover, most hypergravity experiments focus on small-scale systems such as cell cultures or seedlings in petri dishes rather than soil-grown plants [15]–[19]. This gap limits understanding of how hypergravity affects natural soil-plant interactions, including nutrient intake, root behavior, and growth patterns, which are crucial for plant adaptability and stability in both terrestrial and extraterrestrial conditions.

Considering these limitations, this study designed and developed a 1-axis Earth-based hypergravity platform, primarily considering larger chambers that could provide ample space for soil-grown seedlings. Another crucial inclusion in the design is the capability of the growth device's chamber to have a controlled artificial lighting system, in consideration of its power source, wireless controls, and monitoring system. This will allow the investigation of the combined effects of altered gravity and light on seedling development by measuring morphological traits such as main root length (MRL), seminal root count (SRC), dominant seminal root length (DSRL), shoot length (SL), and leaf count (LC).

This study contributes the following: 1) Development of an adjustable Earth-based hypergravity platform for basic experiments on soil-based cultivation of crops that can be grown larger than the scale of a petri dish. This device primarily allows adjusting of gravitational force and light intensity; and 2) Investigation on the combined effects of altered gravity and light intensity on maize root traits such as SRC, DSRL, SL, MRL, and LC, for understanding the potential of maize as a crop that can be cultivated in space.

2 Materials and Methods

This study involves three major technical stages: 1) design and fabrication of a 1-axis Earth-based hypergravity platform, 2) develop the integrated hypergravity speed, irrigation and lighting control systems, and 3) corn cultivation test and measurement of maize seedling morphological traits (Figure 1). ThingSpeak Cloud was instrumentalized to serve as a real-time IoT-based data repository for verification of platform stability and robustness.

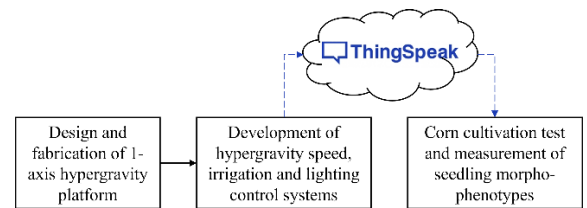


Figure 1: Process flow in developing an Earth-based hypergravity platform to study gravity and light effects on soil-grown seedlings.

2.1 Design and fabrication of earth-based 1-axis hypergravity platform

The selection of materials for fabrication and assembly was based on their physical and mechanical properties, application, availability, and cost. Key factors considered were corrosion and heat resistance, durability, strength, weight, and machining costs. Black iron was chosen for the platform's arms, legs, and frames due to its rigidity, durability, ease of machining, and lower cost compared to aluminum, stainless steel, and galvanized black iron (Figure 2(a)). Carbon steel was used for nuts, bolts, fasteners, and the shaft and bearings because of its high strength and affordability compared to stainless steel. Stainless steel was selected for the electric panel box for its rustproof and moisture-resistant properties, protecting the electronics inside (Figure 2(a)). Aluminum was used for the chamber frame edges, wrapped around PPR plastic, as it is lightweight and more affordable than stainless steel (Figure 2(a)). Polypropylene random copolymer (PPR) plastic was chosen for the chamber housing and sensor cover for its lightweight, corrosion-resistant, and durable properties, making it a better option than PVC, acrylic, or nylon. Polyvinyl chloride (PVC) pipes were used for the chamber cells and water reservoir due to their low cost and lightweight compared to polyethylene (Figure 2(a)). Finally, foam rubber was selected for chamber

padding for its durable cushioning, protecting the chamber cover and body from impact (Figure 2(a)). Shown in Figure 2(b) is the top view of the platform emphasizing the working principle of the hypergravity simulation platform for crop cultivation experiments.

The simulation platform was tested using static and dynamic Finite Element Analysis (FEA) in SolidWorks software to evaluate its load-bearing capabilities [21]. Loads were determined by the weight, based on object density, and centrifugal force from platform rotation. In the static FEA, only Earth's gravitational force (9.81 m/s^2) was applied, with the platform legs set as fixed supports (Figure 2(c)). For dynamic FEA, the motor shaft was fixed for translation but allowed rotation, with platform legs remaining fixed. Motion analysis was also performed to calculate the required power and torque for machine rotation, using the same loads as in dynamic FEA. The shaft was fixed for translation and allowed free rotation, and acceleration was gradually reduced to reach maximum speed after 30 s (Figures 2(c) and (d)).

The hypergravity simulation platform features a DC brushless motor connected to four frames, spaced 90° apart, holding four cultivation chambers (Figure 2(c)). The design was simulated in SolidWorks to ensure a sturdy structure [21]. The platform arms, made from black iron square tubing (1000 mm in length), support the cultivation chambers, which measure $217 \text{ mm} \times 217 \text{ mm} \times 400 \text{ mm}$ and are made from polypropylene board. Inside each chamber, there are nine cells with an area of $1,734.94 \text{ mm}^2$ and a depth of 302 mm, designed for planting seeds. The chamber covers, also made of polypropylene, hold broadband white LED strips to provide light for the crops. The platform's circular plates will be constructed from ASTM A36 steel, while the box compartment for the microcontrollers and other platform parts will be made from AISI 1018 material. Note that the design in this study follows the research group's initial work with improvements in materials selection and rigidity of the entire platform [22].

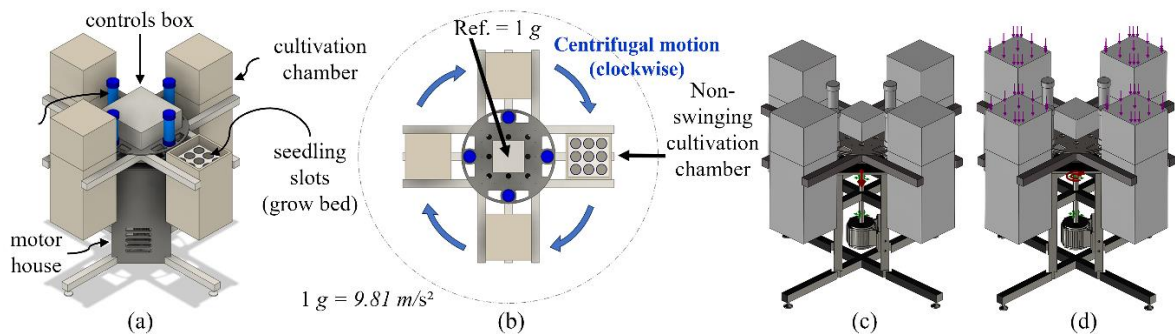


Figure 2: (a) Isometric view of the CAD model for the simulated hypergravity platform. (b) Working principle of the hypergravity simulation platform for crop cultivation experiments. (c) Static finite element analysis and (d) dynamic finite element analysis of the designed platform.

2.2 Development of hypergravity speed, irrigation and lighting control subsystems

This phase involves developing the Arduino-based control systems for hypergravity (speed of the 1-axis rotating platform), irrigation and lighting (Figure 3). This allowed the end-user to configure a certain environmental condition that could affect the growth

of seedlings sown inside the growth chamber including gravity, water availability, and light intensity. On a high-level technical description, the 3-axis digital accelerometer, temperature, humidity, and light intensity sensors were all connected to the ThingSpeak platform for data recording of all three subsystems in Figure 3.

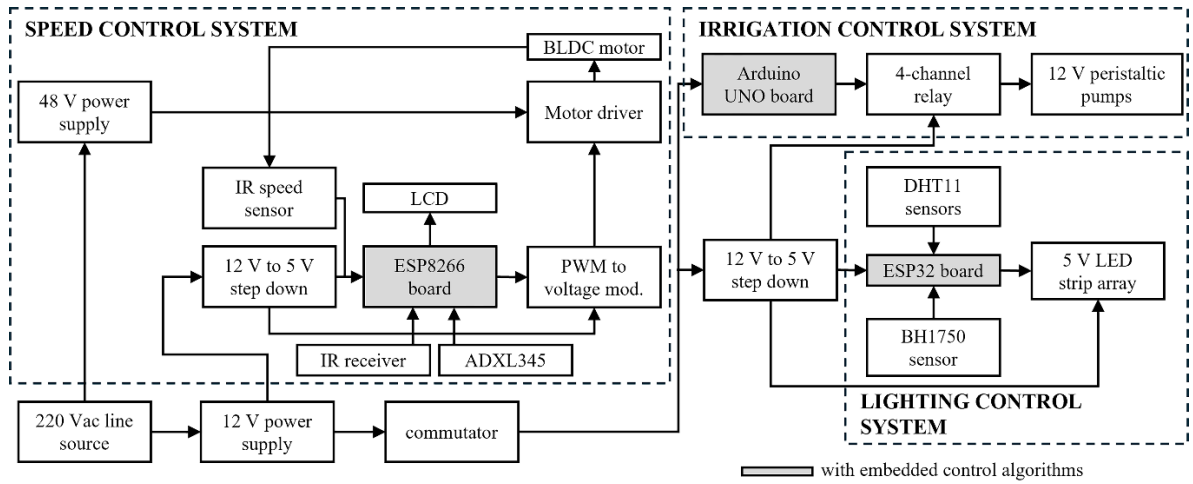


Figure 3: Integrated subsystems diagram for the simulated hypergravity platform for crop seedling cultivation highlighting the speed, irrigation and lighting control systems. All microcontrollers are embedded with control algorithms.

2.1.1 Hypergravity speed control system

To calculate the total mass of the platform, the mass of each part, such as the arms, center squares, chambers, covers, shaft, bearings, water, soil, microcontroller, and drip tubing, was determined by multiplying each part's volume (V) by its density (ρ) expressed in Equation (1). The volume of each part was obtained from SolidWorks, and material densities were referenced from online databases. Miscellaneous parts were assigned a mass of 5 kg. The center circular plates, made of ASTM A36 steel (7850 kg/m^3), had a total volume of 717.27 cm^3 . The shaft and bearings, made of AISI 1018 steel (7870 kg/m^3), had a volume of 215.42 cm^3 . The four hypergravity arms, made of black iron tubes (7870 kg/m^3), had a total volume of 689.85 cm^3 . The four cultivation chambers, made from polypropylene board (920 kg/m^3), had a total volume of 4609 cm^3 . The chamber covers, also made from polypropylene, had a volume of 3066.59 cm^3 . Each reservoir holds 482.31 cm^3 of water, equating to 1.92 kg. Each cell in the cultivation chambers holds 520.48 cm^3 of loam soil (1280 kg/m^3), resulting in a mass of 0.66621 kg per cell. With nine cells per chamber and four chambers, the total soil mass is 23.98 kg. To calculate the minimum required torque for the motor, two key variables were necessary: the moment of inertia of the rotating mass (I) and the angular acceleration of the platform (α), as expressed in Equation (2). The mass moment of inertia of all components with respect to the vertical axis at the point of rotation was obtained using SolidWorks. To

determine the angular acceleration at each g -value for experimentation, Equation (3) was used, requiring angular velocity (ω) and time (t). The platform is designed to accelerate at a constant rate over 30 s, so t is set to 30 s. Equation (4) calculates the angular velocity for each g -value, using the desired g -force (g) and the fixed distance (r) of 40 cm from the axis of rotation to the center of the cultivation chamber (Figure 2(a)). The experiment focuses on achieving 5 g . Using the computed moment of inertia, the required torque for each g -value was calculated and multiplied by an allowance factor of 1.15. This was compared to the actual motor torque using Equation (5).

$$m = V \times \rho \quad (1)$$

$$T = I \times \alpha \quad (2)$$

$$\alpha = \omega / t \quad (3)$$

$$RPM = (g/(r \times 1.118) \times 10^5)^{0.5} \quad (4)$$

$$T = (9550 \times P)/RPM \quad (5)$$

The motor speed control system uses a 12 V power supply converted to 5 V to power the ESP8266 and pulse width modulation (PWM) module (Figure 3). The infrared (IR) remote inputs the desired g -value, which the microcontroller converts to rpm. The PWM is sent to the driver, which controls the motor. An IR sensor monitors rpm, and the microcontroller adjusts the PWM accordingly. At system startup, a g -value is input and converted to rpm. If the motor's PWM is below 240 rpm, the system adjusts the PWM based on the difference between target and actual rpm. If the target rpm exceeds the actual by more than 10, the

PWM increases by one and waits for 1.5 s. For differences under 10 but above 1.5, the PWM increases and waits 8 s. If the difference is less than 1.5, the PWM remains constant for 8 s. When the target rpm value is lower, the process is reversed, decreasing the PWM. Digital accelerometer sensors (ADXL345 model) were attached to the top of three of the chamber covers to measure stability and actual gravity experienced in the growth chamber based on the recommendation in [23].

2.1.2 Irrigation speed control system

The developed irrigation system was a surface drip irrigation system to allow for uniformity in water distribution between each cell. The system consists of the water reservoir, drip hose, peristaltic pump, and 8-way manifold. Each cell in the cultivation chambers contained loam soil and a maize seedling (Figure 2(a)). Each 640 mL of water reservoir was connected to their respective cultivation chambers through a 4/7 mm drip hose. The hose passed through the inlet of the peristaltic pump and the outlet was connected to an 8-way manifold. On the 8-way manifold, only 3 of the 8 outlets were connected to a drip hose line, each aligned to a single column in the cultivation chamber. At each of the three hose lines, small holes were punctured at the location of each cell to allow for water to pass through. The peristaltic pump was activated for a set period of time until each cell received 5 mL of water. The pumps of the irrigation system were powered by a 12 V power supply, which is activated when the relay obtains an input signal from the microcontroller. The control logic has three main variables, initial time off, time, on, and time off. On startup of the prototype, the relay remained off for 10 min to allow for the hypergravity platform to stabilize. After 10 min, the Arduino Uno sends a signal to all four inputs of the relay to activate all four pumps for a period of 40 s. The pumps then remained off for the remainder of the day and continued the cycle daily until the end of testing.

2.1.3 Lighting control system

Artificial photosynthetic light materialized through an LED strip with an RGB setting where equal values of red, blue, and green produce white light. Starting with an initial RGB value close to the desired light intensity, adjustments were made based on sensor readings. If the measured intensity was less than the target and RGB was below 190 digital counts or

intensity level, the values increased. If the measured intensity exceeded the target, the values decreased, provided the difference was under five units. The desired photosynthetic photon flux density in $\mu\text{mol}/\text{m}^2/\text{s}$ was pre-inputted to the ESP32 microcontroller. The LED strips were set to light for an initial of 5 mins and went into a cycle of 8 h off and 16 h on (photoperiod).

2.3 Cultivation test and measurement of seedling morpho-phenotypes

The developed Earth-based hypergravity platform was tested for the viability of crop growth. The glutinous maize genotype “Lagkitan” variant provided by the Bureau of Plant Industry, Manila, was used. Each grow cell in a chamber contained organic loam soil and one maize seed each. Each cell was filled up with loam soil and the seeds were then sown 1 in beneath the soil at an upright angle with the pedicel facing downward. The transparent tape was placed on the bottom of the cell to prevent any possible unabsorbed water from leaking out of the cells during centrifugal simulations. Two cultivation treatments were deployed, namely, control or 1 g treatment (CT), 5 g with 500 lux or $6.80 \mu\text{mol}/\text{m}^2/\text{s}$ (5g500), 5 g with 600 lux or $8.16 \mu\text{mol}/\text{m}^2/\text{s}$ (5g600), 5 g with 700 lux or $9.52 \mu\text{mol}/\text{m}^2/\text{s}$ (5g700), for 5 straight days after sowing (DAS). Three replicates were deployed.

After 5 DAS, seedlings were carefully removed from the soil. Here, the crop phenotypes measured were main root length (MRL), seminal root count (SRC), dominant seminal root length (DSRL), shoot length (SL), and leaf count (LC). All length parameters were measured in mm resolution using a digital ruler. All quantitative data observed in relation to time such as g-value per axis, light intensity, temperature and humidity readings inside the chamber, and delivered water volume per day were all transmitted to and extracted from ThingSpeak in .csv format after every testing period for further analysis. This allowed the visualization of the behavioral trends of the platform in the mentioned parameters over a long period of time and even the analysis of basic averages, minimum, maximum, and standard deviation values.

2.4 Statistical analysis

Pearson Correlation Coefficient (R) presented in a correlogram was generated to establish information about the parametric interrelationships of crop

phenotypes, g-value, and light intensity. In addition, analysis of variance (ANOVA) with significance post-hoc Tukey's test was employed to verify the differences among treatments' data. Both statistical treatments were done using Minitab version 20.4 software [24].

3 Results and Discussion

3.1 Design and operational testing of the 1-axis Earth-based hypergravity platform

With the design of the hypergravity simulation platform and the materials of the components finalized, the total weight of the platform was computed to be 82.68 kg with the weight of the individual chambers being 14.90 kg each (Figure 4(a)).

After conducting static FEA, the factor of safety of the design was found to be 7.6 with a maximum stress of 29 MPa experienced at the arms (Figure 4(b)). Similar to the static FEA results, the maximum stress in dynamic (rotating) conditions occurs at the arms at a value of 86.6 MPa (Figure 4(b)). For the maximum displacement, it radiates outwards from the center of the platform to the edges of the cultivation chambers, reaching a maximum displacement of 2.310 mm which is a negligible amount (Figure 4(c)). The overall factor of safety of the machine was found to be 2.5, indicating the platform is stable enough to withstand the loads applied to it (Figure 4(c)). Based on dynamic analysis, the maximum power needed would be 153 W and the motor torque is 7 N-m, hence, considering the mechanical and electrical efficiency, the motor used in this study is 500 W.

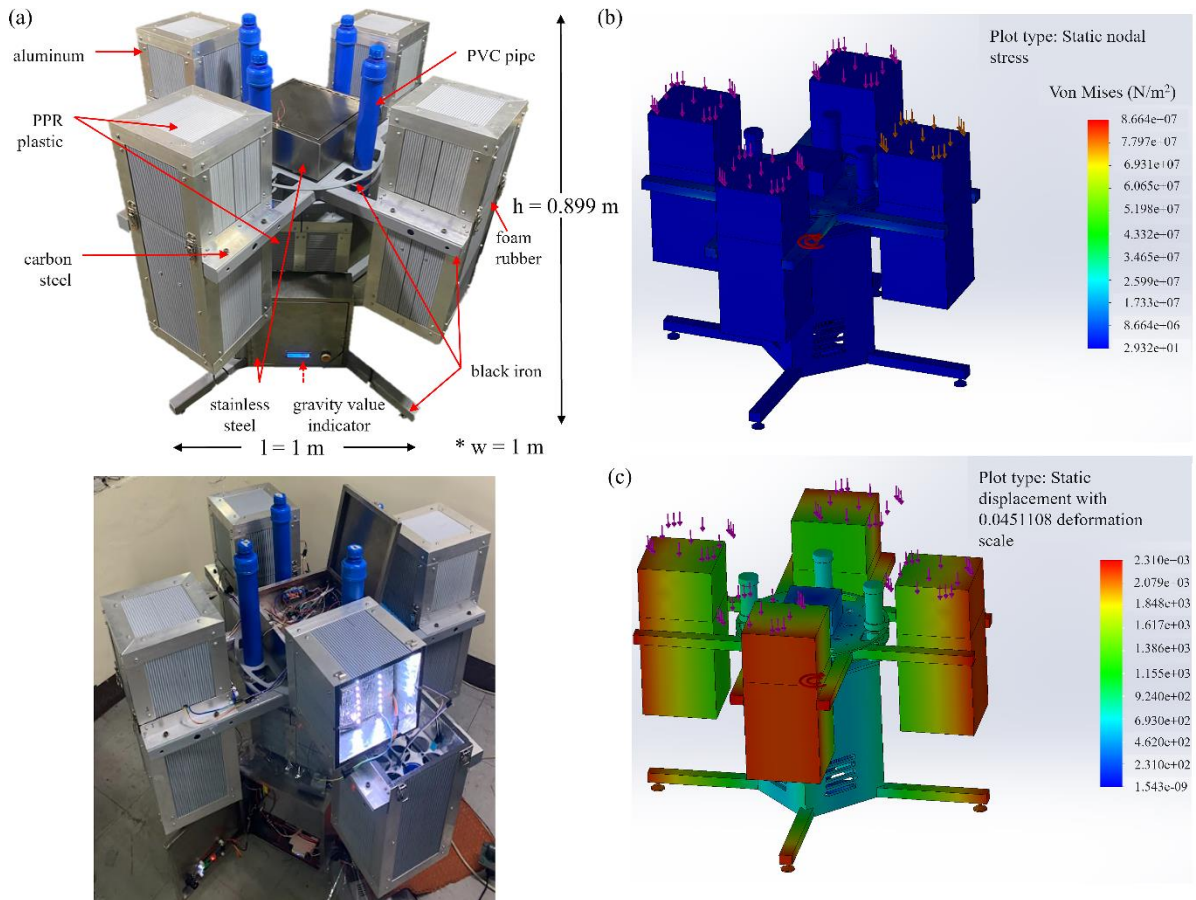


Figure 4: (a) Fabricated Earth-based simulated gravity platform highlighting the exterior and interior sections. Dynamic finite element analysis of the hypergravity platform (b) nodal maximum stress and (c) displacement.

3.2 Performance of hypergravity, irrigation, and lighting control subsystems

The g -values exhibited during actual operation for 5 g in relation to 5g500, 5g600, and 5g700 rotation treatments required a constant motor speed of 105.64 rpm. With the motor which started at rest (speed = 0 rpm), the rotating platform experienced an acceleration phase resulting in g -values less than 5 g at $t = 0$ s to $t = 120$ s at the average (Figure 5(a)). The gravity values measured below 1 g when the platform is operated at the start of 5 g because of dynamic interference where the sensor is subject to vibrations or other accelerations, which often reduce the detected gravitational component. The developed platform is stable at 5 g rotation with an axis-of-interest reading of gravity exertion of 5.012 ± 0.234 g resolution for loaded and unloaded conditions (Figure 5(b)). Loaded means the water reservoir is full of water and the growth chambers are equally filled with soil. In control treatment (rotation at 1 g), the average gravity for each chamber 1 to 4 are 0.985 g , 0.993 g , 1 g , and 0.996 g , respectively, resulting in 0.994 ± 0.008 g resolution. Variations in temperature, humidity, and other environmental factors can impact sensor performance, causing small errors in measurement. The experimental findings for both 1 g (static) and 5 g (dynamic) conditions of the developed simulated gravity platform confirmed their stability during operations and were appropriate for actual seedling cultivation experiments.

Figure 5(c) shows the humidity inside the three used chambers, one for each 5 g cultivation treatment over 5 days. Based on observation, the humidity increased once the irrigation subsystem was activated to water the tubes containing the soil and seedling and decreased over time at a rate of 0.875%/h and increased again after the watering process. However, there is an increase in chamber humidity in DAS 4 and DAS 5, which is potentially due to plant evapotranspiration as the shoot system has already emerged on that day (Figure 5(c)). Although irrigation was an open-loop system, the humidity sensor served to validate that the irrigation system functioned properly and an initial qualitative test through observation was performed and confirmed that soil in each cell was moist after an instance of irrigation cycle without seeds being sown in it. Compared to the test

in 5 g treatments, the humidity inside the chambers for CT did not have a significant increase in humidity outside the time when the irrigation system works. The temperature conditions inside the chambers are similar with a resolution of 25.783 ± 4.5 °C (Figure 5(d)).

The distribution of water for each of the three chambers used during three replicates of 5 g tests resulted in an average of 4.963 mL, 4.824 mL and 4.815 per growth tube, which has corresponding irrigation accuracies of 99.259%, 96.481%, and 96.296%, respectively (Figure 5(e)). Possible reasons for error include the centrifugal force effects, which push water away from the intended path and possibly cause irregular flow rates through the tubes from the water reservoir and the rotation-induced oscillation that affects the stability of water flow, creating brief increases or decreases in the amount of water from the water reservoir reaching the intended soil-filled container. Both causes appeared to increase with distance from the rotation axis and speed of rotation. Hence, with these negligible effects, the developed irrigation system is acceptable for actual seedling cultivation experiments as it can provide enough moisture for seedling growth.

In the design of the experiment of this study, growth chamber 1 was set to light at 6.80 $\mu\text{mol}/\text{m}^2/\text{s}$, chamber 2 at 8.16 $\mu\text{mol}/\text{m}^2/\text{s}$, and chamber 3 at 12.95 $\mu\text{mol}/\text{m}^2/\text{s}$ (Figure 5(f)). The LED strips are designed to light for 5 min at the start to signal that all lights are working appropriately and enter into a loop of turning off for 8 h and on for 16 h. The average light intensity of the LEDs when turned on is 6.81 $\mu\text{mol}/\text{m}^2/\text{s}$, 8.16 $\mu\text{mol}/\text{m}^2/\text{s}$, and 9.52 $\mu\text{mol}/\text{m}^2/\text{s}$ for growth chambers 1 to 3, respectively with corresponding artificial photosynthetic growth light concentration accuracies of 99.918%, 99.960%, and 99.953%. This study demonstrated the design and fabrication of a working simulation platform that enables the analysis of the combined effect of hypergravity and light intensity on crop growth to contribute to the existing space farming studies conducted on Earth (Figures 3 and 4). Overall, the developed hypergravity, irrigation and lighting scheduling and control subsystems exhibited high accuracy for crop seedling growth experimentation in simulated microclimatic conditions. As compared to [17], [18], [20], the current study developed an application-specific hypergravity platform.

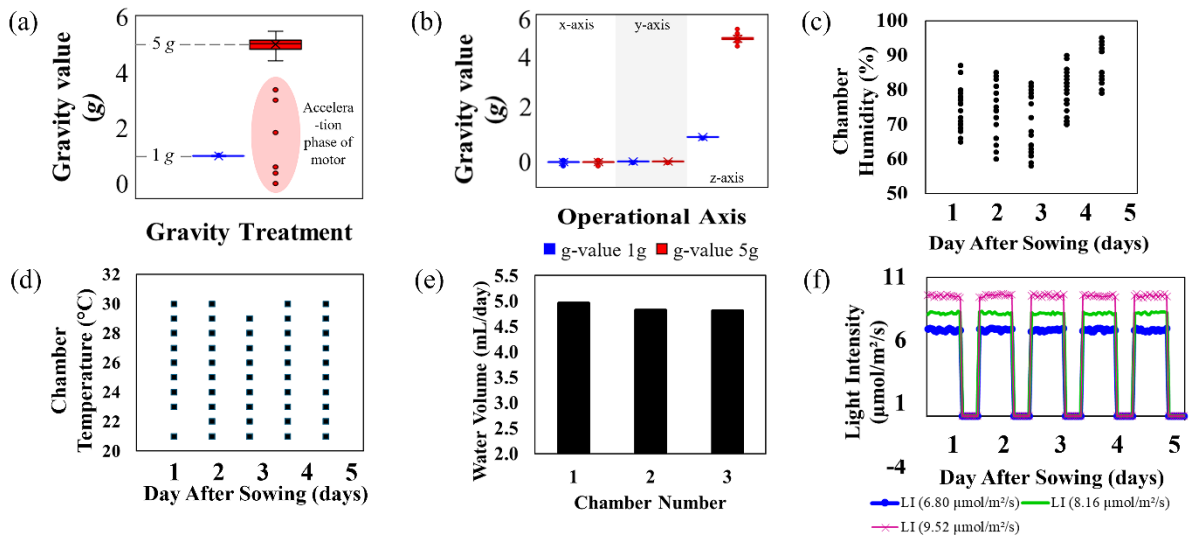


Figure 5: (a) Acceleration phase of motor when operated at 5 g. (b) Stability of gravity control with g-values exhibited on each axis during actual operation. (c)–(d) Internal chamber humidity and temperature. (e) Average injected water volume per growth chamber in 5 g operation with the target of 5 mL/day. (f) Photosynthetic pho control for 6.8 $\mu\text{mol}/\text{m}^2/\text{s}$, 8.16 $\mu\text{mol}/\text{m}^2/\text{s}$ and 9.52 $\mu\text{mol}/\text{m}^2/\text{s}$ per day.

3.3 Seedling growth and morphology

Figure 6(a) and (b) show the representative maize seedling samples cultivated in 1 g and 5 g treatments for 5 continuous days that are still in place with the grow tubes inside the growth chamber and the extracted whole seedling structure. All treatments (CT and 5 g exposed with 6.8 $\mu\text{mol}/\text{m}^2/\text{s}$, 8.16 $\mu\text{mol}/\text{m}^2/\text{s}$ and 9.52 $\mu\text{mol}/\text{m}^2/\text{s}$) exhibited 100% germination of maize seedlings. It was observed that seedlings grown in 5 g and 6.8 $\mu\text{mol}/\text{m}^2/\text{s}$ of white light (5g500 treatment) had significantly reduced major root length, dominant seminal root length, and shoot length, compared to seedlings that received higher light intensity (8.16 $\mu\text{mol}/\text{m}^2/\text{s}$ and 9.52 $\mu\text{mol}/\text{m}^2/\text{s}$). On the other hand, the seedlings grown at 5 g and 8.16 $\mu\text{mol}/\text{m}^2/\text{s}$ exhibited the least growth in terms of seminal root count and leaf count. Specifically, the 5 g treatment with 6.8 $\mu\text{mol}/\text{m}^2/\text{s}$ resulted in 163.444 \pm 80 mm for MRL, 5 \pm 2 for SRC, 91.222 \pm 46 mm for DSRL, 78.778 \pm 35 mm for SL, and an average of one fully open leaf. The 5 g treatment with 8.16 $\mu\text{mol}/\text{m}^2/\text{s}$ resulted in 182.333 \pm 3.778 mm for MRL, 3 \pm 1 for SRC, 95.667 \pm 63 mm for DSRL, 100.111 \pm 37 mm for SL, and an average of one fully open leaf. The 5 g treatment with 9.52 $\mu\text{mol}/\text{m}^2/\text{s}$ resulted in 172.667 \pm 50.5 mm for MRL, 4 \pm 1 for SRC, 106.778 \pm 37.5 mm for DSRL, 87.722 \pm 23.5 mm for SL and an average of one fully open leaf. The seedlings at 5 g, which received the highest light intensity (9.52 $\mu\text{mol}/\text{m}^2/\text{s}$)

exhibited the longest dominant seminal root length and a consistent number of leaves per seedling. Unlike the 5 g treatments, it was observed that seedlings cultivated in 1 g with 9.52 $\mu\text{mol}/\text{m}^2/\text{s}$ of white light (1g700 treatment) had significantly reduced the major root length, dominant seminal root length, and shoot length, compared to seedlings that received lower light concentrations (6.8 $\mu\text{mol}/\text{m}^2/\text{s}$ and 8.16 $\mu\text{mol}/\text{m}^2/\text{s}$). On the other hand, the seedlings grown in 1 g and 9.52 $\mu\text{mol}/\text{m}^2/\text{s}$ exhibited the least growth in seminal root count. Specifically, the 1 g treatment with 6.8 $\mu\text{mol}/\text{m}^2/\text{s}$ resulted in 181.111 \pm 54 mm for MRL, 4 \pm 1 for SRC, 179.778 \pm 55.5 mm for DSRL, 149.556 \pm 34 mm for SL, and an average of one fully open leaf at DAS 5. The 1 g treatment with 8.16 $\mu\text{mol}/\text{m}^2/\text{s}$ resulted in 163.667 \pm 66.5 mm for MRL, 3 \pm 1 for SRC, 185.444 \pm 39 mm for DSRL, 144.778 \pm 29.5 mm for SL, and an average of one fully open leaf. The 1 g treatment with 9.52 $\mu\text{mol}/\text{m}^2/\text{s}$ resulted in 152.444 \pm 58.5 mm for MRL, 4 \pm 1 for SRC, 172.944 \pm 55 mm for DSRL, 140.333 \pm 32.5 mm for SL and an average of one fully open leaf.

These findings imply that root and shoot traits are sensitive to both gravity and light intensity, each influencing growth patterns differently [6]. In 5 g environments, higher light intensity (closer to 9.52 $\mu\text{mol}/\text{m}^2/\text{s}$) may be beneficial for optimal root elongation and shoot development. In a 1 g (Earth gravity) environment, moderate light (6.8–8.16 $\mu\text{mol}/\text{m}^2/\text{s}$) appears more suitable to avoid growth

limitations, particularly in root traits, as $9.52 \mu\text{mol}/\text{m}^2/\text{s}$ appeared to be excessive for the selected maize genotype. The optimal light intensity for root and shoot development appears to differ between gravity levels, with 5 g seedlings benefiting from higher light exposure (up to $9.52 \mu\text{mol}/\text{m}^2/\text{s}$) for root elongation and shoot growth, while 1 g seedlings perform best at moderate light levels. The differential response highlights the importance of fine-tuning light exposure based on gravity conditions to achieve balanced growth in controlled environments, potentially informing strategies for plant cultivation in space or other low- and high-gravity conditions.

The seminal root count of maize increases by a rate of 1.457 root/g and $0.536 \text{ root}/\mu\text{mol}/\text{m}^2/\text{s}$ increase (Figure 6(c)). The dominant seminal root length increases by a rate of 46.213 mm/g and $11.996 \text{ mm}/\mu\text{mol}/\text{m}^2/\text{s}$ increase (Figure 6(d)). The shoot length increases by a rate of 38.960 mm/g and $6.112 \text{ mm}/\mu\text{mol}/\text{m}^2/\text{s}$ increase (Figure 6(e)). The major root length (radicle) increases by a rate of 56.426 mm/g and $21.178 \text{ mm}/\mu\text{mol}/\text{m}^2/\text{s}$ increase (Figure 6(f)). And leaf count increases by a rate of 0.321 leaf/g and $0.077 \text{ leaf}/\mu\text{mol}/\text{m}^2/\text{s}$ increase (Figure 6(g)). Both gravity and light intensity positively influence root and shoot traits in maize, with gravity exerting a greater effect across traits (Figure 6(h)). Root and shoot elongation showed higher sensitivity to gravitational increases, which could inform strategies for optimizing plant growth in various environments by adjusting gravity and light levels. Light intensity still contributes to growth across traits, especially for traits like dominant seminal root length and shoot length but may play a secondary role compared to gravity [20].

3.4 Parametric interrelationships of crop phenotypes

From the combined 1 g and 5 g experimental dataset measured during the 5 days triplicate experiments, it was confirmed that gravity has a strong negative correlation with the dominant seminal root length, shoot length and leaf count, while it has a negligible effect on the main root length and seminal root count (Figure 7). There is a computed p -value of 0.008 that is significantly less than the α of 0.05, thus, strong evidence that CT and hypergravity groups have

comparably different means, especially in DSRL, MRL, SL, and LC root features (Table 2). The white light intensity negatively affects the major root length and seminal root count and is almost negligible to the growth of the dominant seminal root length and shoot length. Also, it has a weak positive correlation with the maturation of the leaf referring to leaf count (Figure 7). Interestingly, under the combined varied gravity and photosynthetic photon flux density settings, when shoot length increases, the dominant seminal root length increases, and the leaf count has a tendency to increase as well. This implies that with increased shoot length, the plant can absorb more light, thereby enhancing photosynthesis. This additional energy enables further root growth including dominant seminal roots as the plant seeks to support the larger shoot system. Increased leaf count can also be a byproduct of higher photosynthetic rates, as more leaves enable further light capture and growth [25]. Roots respond strongly to gravity, which causes a redistribution of auxin toward the lower side of the root, supporting longer root structures like the dominant seminal root [20]. This response ensures the plant has adequate root length to support water and nutrient uptake as shoot growth demands increase.

The supply of resources would gradually decrease over time with long and continuous extraterrestrial explorations [26]. Understanding the effects of altered gravity and light on crop growth will help sustain long-term space inhabitation and farming by astronauts, especially since there are multiple different occurrences of hypergravity, namely during the launch and re-entry of spacecraft, in regions close to black holes, simulators aboard the spacecraft, and planets with a gravitational pull greater than 1 g [27]. Investigations on the effect of hypergravity on maize growth and morphology can have a scientific impact as it contributes to the few known literature on plant growth under hypergravity [28]. It is also possible to extrapolate responses to altered gravity based on the gravity continuum principle and reduced gravity paradigm under the right situations of hypergravity [26]. Similarly, this study has a technological impact because it includes developing a system that simulates space conditions instead of traveling to any region along the lower earth orbit or outer space [29].

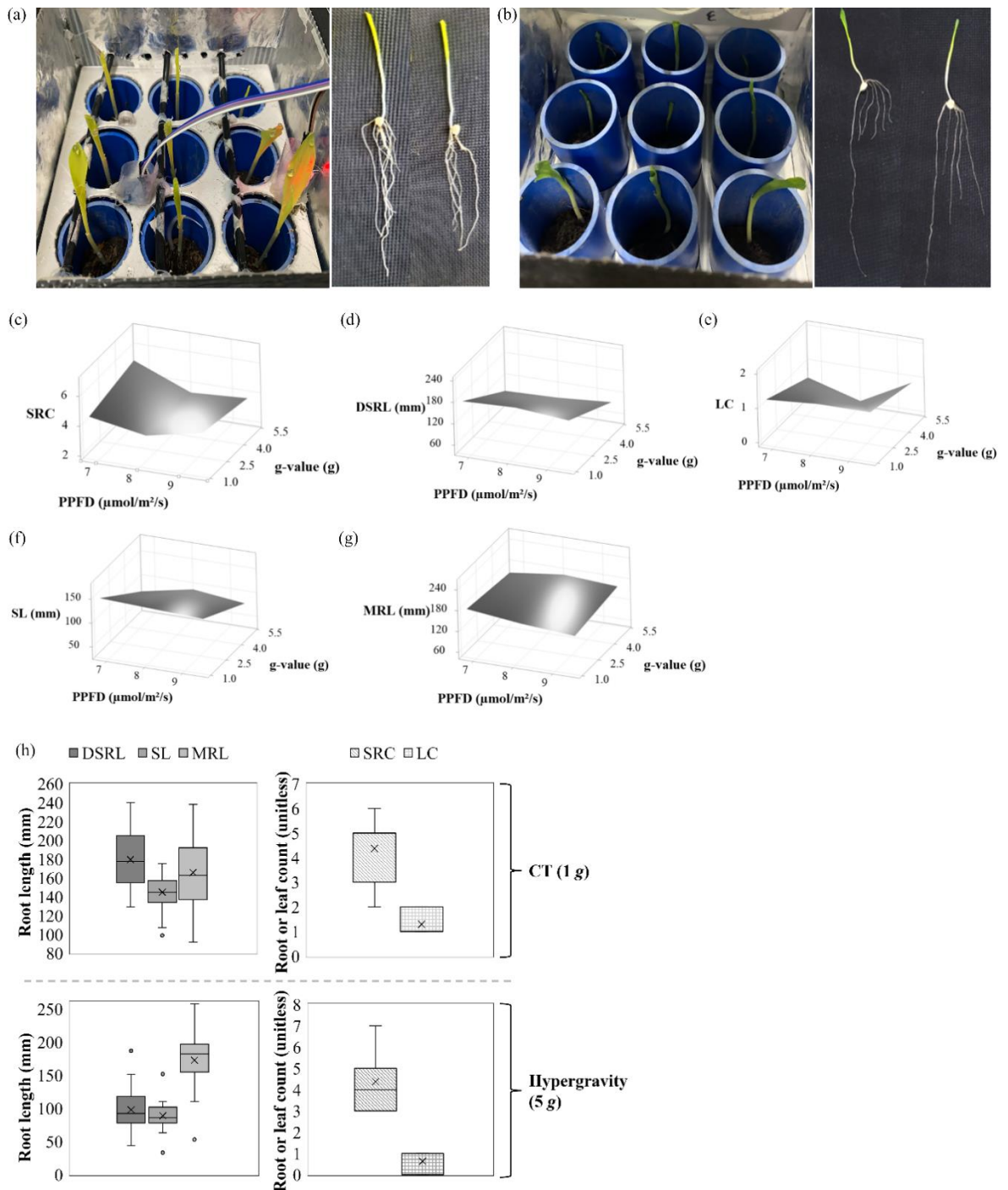
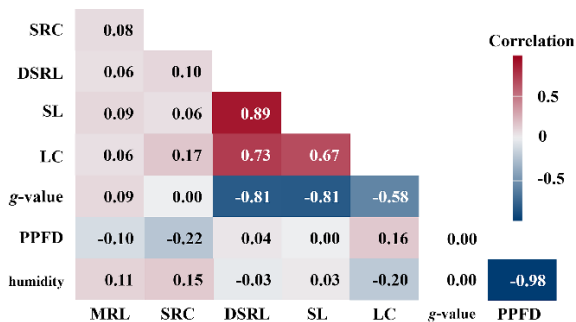


Figure 6: Representative maize seedling samples cultivated in (a) 1 g and (b) 5 g treatments for 5 continuous days. Dynamics of maize (c) seminal root count (SRC), (d) dominant seminal root length (DSRL), (e) shoot length (SL), (f) major root length (MRL), (g) leaf count (LC) in relation to varied gravity and photosynthetic photon flux density, and (h) the variations in DSRL, SL, MRL, SRC and LC with respect to control (CT) and hypergravity treatments.



The initial findings about correlations are supported by the findings of post-hoc Tukey's test in Table 1 where the dominant seminal root length and major root length have homogenous patterns in 1 g treatment and major root length possibly to establish a balanced and stable root system for nutrient uptake and plant support. A similar pattern in growth for major root length and shoot length might indicate an adaptive response where both root and shoot growth are aligned to support the plant's structural stability in hypergravity. The findings of this study are in agreement that increased gravity can enhance root system robustness while potentially limiting shoot elongation to prevent tipping or mechanical stress [30].

Figure 7: Correlations of maize seedling phenotypes with varying g -value and light intensity during cultivation.

Table 1: Grouping information using Tukey's post-hoc test and 95% confidence ANOVA.

Gravity Treatment	Mean				
	DSRL (mm)	MRL (mm)	SL (mm)	SRC (mm)	LC (mm)
CT (1 g)	179.390 ^a	165.740 ^a	144.890 ^b	4.370 ^c	1.296 ^c
Hypergravity (5 g)	172.810 ^a	97.890 ^b	88.970 ^b	4.370 ^c	0.630 ^c

^{a,b} are Tukey grouping labels where mean values followed by the same letter are not significantly different at $p < 0.05$

The development of the irrigation system aided and boosted maize's growth based on root and shoot growth. Shown in Table 2 is the comparison of the proposed study to other related studies with custom-built altered gravity Earth-based platforms for crop cultivation testing in hypergravity [20], [31], [32]. The Large Diameter Centrifuge of ESA can be monitored using LabView protocols [20]. Interestingly, there are calcium-sensitive fluorescent indicators such as aequorin-based luminescence measurement for real-time calcium imaging in the root of *Arabidopsis* seedlings [31]. Through this simulation, hypergravity was found to induce transient improvements in intracellular calcium concentration suggesting that calcium signaling is gravity-dependent. The *Physcomitrella patens* grew faster and produced more biomass under 2.3 to 10 g suggesting that for this plant

species, the photosynthetic activity is gravity-dependent [32]. More than this, the current study confirms that crops, such as *Zea mays* can perceive and naturally respond to gravitational forces specially expressed through their root growth and architecture. Unlike [20], [31], [32], the current study highlighted the combined interaction of gravity and light intensity for both root and shoot systems giving way to implications for optimizing plant growth in space environments not only to potential space food but also for sustainable bioregenerative life support systems. The innovative simulated gravity device developed in this study offers a scalable solution for future research on plant cultivation in controlled gravity environments, making it valuable for advancements in space agriculture.

Table 2: Comparison of the proposed study to other related studies with custom-built altered gravity Earth-based platform for crop cultivation testing in hypergravity.

Gravity Value Range (g)	Platform's Degree-of-Freedom	Growth Chamber Count	Max. Seedling Count Per Chamber	Crop Tested	Growth Media	Controlled Tropistic Stimulus Included	Focused Plant Tropism	Reference
1 – 20	1	2	6	<i>Arabidopsis thaliana</i>	Agar	Gravity and light intensity	Root	[31]
2.3 – 10	1	1	Not specified	<i>Physcomitrella patens</i>	Agar	Gravity	Shoot	[32]
1 – 20	3	4	25	<i>Brassica oleracea</i>	Gel	Gravity and light spectrum	Root	[20]
1 – 5	1	4	9	<i>Zea mays</i>	Soil	Gravity and light intensity	Root and shoot	This study

4 Conclusions

The custom-built 1-axis hypergravity platform developed in this study successfully enabled controlled cultivation of soil-grown maize seedlings under variable gravity and light conditions, which allows for advancing our understanding of plant responses in non-terrestrial environments. By accommodating larger plants, this platform demonstrated that hypergravity has significant effects on root and shoot traits, with light intensity also modulating these responses. The platform's wireless controls and adjustable lighting systems enabled precise environmental manipulation, establishing it as an effective tool for exploring crop growth adaptability in both terrestrial and extraterrestrial applications. This study demonstrates that maize seedlings exhibit distinct growth responses to combined hypergravity and varying light intensities, with gravity exerting a primary influence on root and shoot traits. A hypergravity environment at 5 g was found to benefit from higher light intensities for optimal growth, while moderate light was preferable in 1 g conditions to prevent growth limitations. Light intensity and gravity interact to influence developmental outcomes, with increased shoot growth enabling more photosynthesis, which in turn supports greater root development. These findings suggest that fine-tuning gravity and light exposure can optimize plant growth, with implications for controlled agricultural systems in both terrestrial and extraterrestrial settings. Such adaptive growth responses highlight the need to consider both gravitational and lighting factors when designing growth chambers for space agriculture, contributing to future strategies in crop cultivation under variable gravity. For future works, to improve the hypergravity platform, the cultivation chambers should be modified for taller crops, allowing growth beyond the seedling stage for more comprehensive observations. Replacing vertical chambers with horizontal ones may reveal how chamber orientation impacts growth under centrifugal force. Integrating solenoid valves into the irrigation system and testing various crop types would further enhance space agriculture research by identifying crops resilient to hypergravity. Additionally, repositioning the light source within each chamber could yield insights into phototropic responses under altered gravity conditions.

Acknowledgments

This study is supported by the Department of Science and Technology – Engineering Research and Development for Technology (DOST-ERDT) of the Philippines and the De La Salle University, Manila. The authors would like to thank Dr. Luigi Gennaro Izzo from the University of Naples Federico II, Portici, Italy, for the suggestions for improving the technical contents of this article.

Author Contributions

M.J.D.: conceptualization, investigation, methodology, writing an original draft, research design, data analysis, data curation; M.A.: conceptualization, investigation, methodology, writing an original draft, research design; J.R.L.: conceptualization, investigation, methodology, writing an original draft, research design, data curation; J.R.: conceptualization, investigation, methodology, writing an original draft, research design; J.M.T.: conceptualization, investigation, methodology, writing an original draft, research design; R.C.: conceptualization, investigation, reviewing and editing, methodology, research design, data analysis, writing—reviewing and editing, project administration; R.R.: conceptualization, reviewing and editing, methodology, writing—reviewing and editing. All authors have read and agreed to the published version of the manuscript.

Conflicts of Interest

The authors declare no conflict of interest.

References

- [1] G. Pozhvanov and D. Suslov, “Sucrose and mannans affect arabidopsis shoot gravitropism at the cell wall level,” *Plants*, vol. 13, no. 2, 2024, doi: 10.3390/plants13020209.
- [2] X. Xia, X. Mi, L. Jin, R. Guo, J. Zhu, H. Xie, L. Liu, Y. An, C. Zhang, C. Wei, and S. Liu, “CsLAZY1 mediates shoot gravitropism and branch angle in tea plants (*Camellia sinensis*),” *BMC Plant Biology*, vol. 21, no. 1, 2021, doi: 10.1186/s12870-021-03044-z.
- [3] K. Retzer and W. Weckwerth, “Recent insights into metabolic and signalling events of directional root growth regulation and its implications for sustainable crop production

- systems,” *Frontiers in Plant Science*, vol. 14, pp. 249–256, 2023, Art. no. 1154088, doi: 10.3389/fpls.2023.1154088.
- [4] S. Harmer and C. Brooks, “Growth-mediated plant movements: Hidden in plain sight,” *Current Opinion in Plant Biology*, vol. 41, pp. 89–94, 2018, doi: 10.1016/j.pbi.2017.10.003.
- [5] H. Han, M. Adamowski, L. Qi, S. S. Alotaibi, and J. Friml, “PIN-mediated polar auxin transport regulations in plant tropic responses,” *New Phytologist*, vol. 232, no. 2, pp. 510–522, 2021, doi: 10.1111/nph.17617.
- [6] K. Hamann, M. Meier, N. Lewis, and A. Carim, “Plastic morphological response to spectral shifts during inorganic phototropic growth,” *JACS Au*, vol. 2, no. 4, pp. 865–874, 2022, doi: 10.3732/ajb.
- [7] X. Qian, Y. Zhao, Y. Alsaid, X. Wang, M. Hua, T. Galy, H. Gopalakrishna, Y. Yang, J. Cui, N. Liu, M. Marszewski, L. Pilon, H. Jiang, and X. He, “Artificial phototropism for omnidirectional tracking and harvesting of light,” *Nat Nanotechnology*, vol. 14, no. 11, pp. 1048–1055, 2019, doi: 10.1038/s41565-019-0562-3.
- [8] Y. Zhang, J. Lu, and Y. He, “Long-term partial gravity environment simulation method based on double inclined and horizontal planes cyclical simulation device,” *Measurement*, vol. 202, 2022, Art. no. 111830, doi: 10.1016/j.measurement.2022.111830.
- [9] L. E. Romano, J. J. W. A. van Loon, L. G. Izzo, M. Iovane, and G. Aronne, “Effects of altered gravity on growth and morphology in *Wolffia globosa* implications for bioregenerative life support systems and space-based agriculture,” *Scientific Reports*, vol. 14, no. 410, 2024, doi: 10.1038/s41598-023-49680-3.
- [10] V. D. Micco, G. Aronne, N. Caplin, E. Carnero-Diaz, R. Herranz, N. Horemans, V. Legue, F. J. Medina, V. Pereda-Loth, M. Schiefloe, S. De Francesco, L. G. Izzo, I. Le Disquet, and A. K. Jost, “Perspectives for plant biology in space and analogue environments,” *npj Microgravity*, vol. 9, no. 67, 2023, doi: 10.1038/s41526-023-00315-x.
- [11] R. Hosamani, B. K. Swamy, A. Dsouza, and M. Sathasivam, “Plant responses to hypergravity: A comprehensive review,” *Planta*, vol. 257, no. 17, 2023, doi: 10.1007/s00425-022-04051-6.
- [12] Y. Makino, K. Ichinose, M. Yoshimura, Y. Kawahara, and L. Yuge, “Efficient preservation of sprouting vegetables under simulated microgravity conditions,” *PLoS One*, vol. 15, no. 10, 2020, doi: 10.1371/journal.pone.0240809.
- [13] L. T. Bien, T. T. Hoang, M. Nguyen, T. H. Phong, D. M. Cuong, H. D. Khai, V. M. Luan, N. B. Nam, T. Trinh, B. V. T. Vinh, and N. D. Tan, “Morphogenesis of in vitro strawberry leaf cultured under clinostat 2D condition,” *Plant Cell Tissue and Organ Culture*, vol. 153, no. 3, pp. 499–510, 2023, doi: 10.1007/s11240-023-02484-9.
- [14] M. A. Valbuena, A. Manzano, J. P. Vandenbrink, V. Pereda-Loth, E. Carnero-Diaz, R. E. Edelmann, J. Z. Kiss, R. Herranz, and F. Javier Medina, “The combined effects of real or simulated microgravity and red-light photoactivation on plant root meristematic cells,” *Planta*, vol. 248, no. 3, pp. 691–704, 2018, doi: 10.1007/s00425-018-2930-x.
- [15] Q. S. Wang, M. H. Li, and D. W. Li, “Solitary wave generation and propagation under hypergravity fields,” *Water (Switzerland)*, vol. 10, no. 10, 2018, doi: 10.3390/w10101381.
- [16] A. Kume, H. Kamachi, Y. Onoda, Y. Hanba, Y. Hiwatashi, I. Karahara, and T. Fujita, “How plants grow under gravity conditions besides 1 g: Perspectives from hypergravity and space experiments that employ bryophytes as a model organism,” *Plant Molecular Biology*, vol. 107, pp. 279–291, 2021, doi: 10.1007/s11103-021-01146-8.
- [17] S. Brungs, G. Petrat, M. von der Wiesche, R. Anken, W. Kolanus, and R. Hemmersbach, “Simulating parabolic flight like g-profiles on ground - A combination of centrifuge and clinostat,” *Microgravity Science and Technology*, vol. 28, no. 3, pp. 231–235, 2016, doi: 10.1007/s12217-015-9458-5.
- [18] N. de Sous, G. Rodriguez-Esteban, I. Colage, P. D’Ambrosio, J. J. W. A. van Loon, E. Salo, T. Adell, and G. Auletta, “Transcriptomic analysis of planarians under simulated microgravity or 8 g demonstrates that alteration of gravity induces genomic and cellular alterations that could facilitate tumoral transformation,” *International Journal of Molecular Sciences*, vol. 20, no. 3, 2019, doi: 10.3390/ijms20030720.
- [19] T. Frett, G. Petrat, J. J. Jack, R. Hemmersbach, and R. Anken, “Hypergravity facilities in the ESA ground-based facility program – Current research activities and future tasks,” *Microgravity Science and Technology*, vol. 28,

- no. 3, pp. 205–214, 2016, doi: 10.1007/s12217-015-9462-9.
- [20] J. J. W. A. van Loon, J. Krause, H. Cunha, J. Goncalves, H. Almeida, and P. Schiller, “The large diameter centrifuge, LDC, for life and physical sciences and technology,” in *Proceedings of the Life in Space for Life on Earth Symposium*, vol. 553, p. 92, 2008.
- [21] Dassault Systèmes. *SolidWorks 2023*. (2023). Accessed: Dec. 12, 2024. [Online]. Available: <https://www.solidworks.com>
- [22] M. J. C. Dionel, M. P. Alaan, J. A. Lato, J. Reyes, J. M. Tan, R. Concepcion II, R. Relano, and A. Bandala, “Optimization of a hypergravity platform design for earth-based astrobotany applications using finite element analysis,” in *2023 IEEE 15th International Conference on Humanoid, Nanotechnology, Information Technology, Communication and Control, Environment, and Management (HNICEM)*, 2023, doi: 10.1109/HNICEM60674.2023.10589090.
- [23] M. J. Dionela, J. M. Tan, L. M. Paran, R. Concepcion II, A. Bandala, and L. G. Izzo, “Design of a hypergravity simulation platform with speed and axis stability control systems,” in *2022 IEEE 14th International Conference on Humanoid, Nanotechnology, Information Technology, Communication and Control, Environment, and Management (HNICEM)*, 2022, doi: 10.1109/HNICEM57413.2022.10109584.
- [24] M. Sathasivam, R. Hosamani, B. K. Swamy, and S. Kumaran, “Plant responses to real and simulated microgravity,” *Life Sciences in Space Research*, vol. 28, pp. 74–86, 2021, doi: 10.1016/j.lssr.2020.10.001.
- [25] Minitab LLC. *Minitab 21*. (2023). Accessed: Dec. 12, 2024. [Online]. Available: <https://www.minitab.com>
- [26] C. Wade, “Responses across the gravity continuum: Hypergravity to microgravity,” *Advances in Space Biology and Medicine*, vol. 10, pp. 225–245, 2005, doi: 10.1016/S1569-2574(05)10009-4.
- [27] L. E. Romano, J. J. W. A. van Loon, L. G. Izzo, M. Iovane, and G. Aronne, “Effects of altered gravity on growth and morphology in *Wolffia globosa* implications for bioregenerative life support systems and space-based agriculture,” *Scientific Reports*, vol. 14, no. 410, 2024, doi: 10.1038/s41598-023-49680-3.
- [28] K. H. Hasenstein and J. J. W. A. van Loon, “Clinostats and other rotating systems-design, function, and limitations,” *Generation and Applications of Extra-Terrestrial Environments on Earth*, vol. 6, pp. 147–156, 2015.
- [29] M. Calvaruso, C. Militello, L. Minafra, V. La Regina, F. Torrisi, G. Pucci, F. P. Cammarata, V. Bravata, G. I. Fote, and G. Russo, “Biological and mechanical characterization of the Random Positioning Machine (RPM) for microgravity simulations,” *Life (Basel)*, vol. 11, no. 11, 2021, doi: 10.3390/life11111190.
- [30] M. Toyota and S. Gilroy, “Gravity and mechanical signaling in plants,” *American Journal of Botany*, vol. 100, no. 1, pp. 111–125 2013, doi: 10.3732/ajb.1200408.
- [31] M. Toyota, T. Furuichi, H. Tasumi, and M. Sokabe, “Hypergravity stimulation induces changes in intracellular calcium concentration in *Arabidopsis* seedlings,” *Advances in Space Research*, vol. 39, pp. 1190–1197, 2007, doi: 10.1016/j.asr.2006.12.012.
- [32] K. Takemur, H. Kamachi, A. Kume, T. Fujita, I. Karahara, and Y. T. Hanba, “A hypergravity environment increases chloroplast size, photosynthesis, and plant growth in the moss *Physcomitrella patens*,” *Journal of Plant Research*, vol. 130, pp. 181–192, 2017, doi: 10.1007/s10265-016-0879-z.